Int. J. Anal. Appl. (2026), 24:247

International Journal of Analysis and Applications

Inverse Source Reconstruction in a Space–Time Fractional Diffusion Model with Variable-Order Caputo Derivative from Terminal Observations

Eman Alruwaili*

Department of Mathematics, College of Science, Northern Border University, Arar, Saudi Arabia

Corresponding author: Iman.Alrowili@nbu.edu.sa

Abstract. This paper investigates an inverse source problem for a space–time fractional diffusion equation involving a spectral fractional Laplacian in space and a variable-order Caputo derivative in time. The goal is to reconstruct an unknown spatial source term from terminal-time observations, a setting that is known to be severely ill-posed due to the strong smoothing effect of the underlying diffusion operator. From a theoretical perspective, we first establish the well-posedness of the associated forward problem in an appropriate fractional energy framework, under an explicit structural hypothesis on the variable-order Caputo derivative that is known to hold in the constant-order case and under additional regularity conditions in the genuinely variable-order case. The inverse problem is then reformulated as a linear operator equation, and its identifiability is rigorously analyzed under a companion positivity hypothesis. In particular, we provide a spectral characterization of the forward operator, which allows us to explicitly explain the mechanism of instability through the decay of modal coefficients. On the computational side, we propose an iterative reconstruction approach based on the conjugate gradient method combined with Morozov's discrepancy principle, providing an effective regularization strategy without requiring explicit tuning of regularization parameters. The space operator is discretized using a spectral method, while the variable-order Caputo derivative is approximated by an L1-type scheme adapted to time-dependent fractional orders. The main novelty of this work lies in the unified treatment of variable-order time-fractional dynamics and inverse source reconstruction in one-dimensional settings, together with a comparison against the constant-order model; the two-dimensional experiment illustrates the reconstruction method but does not itself constitute a variable-versus-constant order comparison. Numerical experiments, including challenging nonsmooth sources and multiple noise levels, demonstrate that the proposed method is stable and accurate. The results indicate that, while variable-order effects introduce additional modeling flexibility, the reconstruction quality is predominantly governed by the noise level and the intrinsic ill-posedness of the problem.

1. Introduction

Fractional diffusion equations have emerged as a powerful modeling framework for describing anomalous transport phenomena that cannot be adequately captured by classical integer-order

Received: May 1, 2026.

2020 *Mathematics Subject Classification.* 35R30.

Key words and phrases. inverse source problem; variable-order fractional diffusion; conjugate gradient method.

https://doi.org/10.28924/2291-8639-24-2026-247
ISSN: 2291-8639

models. Such phenomena arise naturally in a wide range of applications, including porous media flow, viscoelastic materials, biological systems, and complex heterogeneous environments. Unlike standard diffusion equations, fractional models incorporate memory effects and nonlocal spatial interactions, typically through Caputo-type time derivatives and fractional Laplacian operators [1–6]. In many practical situations, certain parameters or source terms appearing in the governing equations are not directly observable and must be reconstructed from indirect measurements. This leads to inverse problems, which are well known to be ill-posed in the sense of Hadamard, meaning that small perturbations in the data may produce large deviations in the reconstructed quantities. Consequently, the analysis and numerical solution of inverse problems for fractional diffusion equations have attracted significant attention over the past decade [7–9]. For constant-order fractional diffusion equations, a considerable body of literature has been devoted to inverse source identification problems using various types of measurements, including final-time data and integral observations. Theoretical results on uniqueness and stability, as well as numerical reconstruction methods based on regularization techniques, have been established in several works [10–12]. In particular, optimization-based approaches such as Tikhonov regularization and conjugate gradient methods have proven effective in recovering spatial source terms in fractional diffusion models. More recently, increasing attention has been directed toward variable-order fractional models, in which the fractional order depends on time or space. These models provide additional flexibility for describing complex physical processes with evolving memory effects. However, inverse problems for variable-order fractional diffusion equations remain relatively less explored and present additional mathematical and numerical challenges due to the time-dependent nature of the fractional operator; in particular, it is by now well documented that the variable-order Caputo derivative does not enjoy the time-translation-invariant convolution structure of its constant-order counterpart, so that several classical energy and comparison estimates require dedicated (and sometimes structurally corrected) proofs rather than a direct transcription of the constant-order arguments. Recent contributions in this direction include inverse problem and stability analysis for variable-order diffusion equations [13–15]. On the numerical side, several methods have been proposed for solving inverse problems in fractional diffusion equations, including iterative regularization methods, quasi-boundary value methods, and adjoint-based optimization techniques. However, most existing studies focus on one-dimensional problems or constant-order models, while multidimensional inverse problems involving nonlocal fractional operators remain comparatively underdeveloped. Motivated by these challenges, in this work we study an inverse source problem for a space–time fractional diffusion model involving a fractional Laplacian and a time-dependent fractional order. The objective is to reconstruct an unknown spatial source term from terminal observations. The problem is formulated within a rigorous functional framework, and the corresponding forward problem is first analyzed to establish well-posedness of weak solutions under an explicit structural hypothesis (Assumption 2.1) on the variable-order Caputo derivative. The inverse problem is then investigated, and theoretical properties such as uniqueness and stability are discussed under this hypothesis together with a companion positivity hypothesis (Assumption 3.2). From a computational perspective, the reconstruction is formulated as a regularized optimization problem, which is solved using a conjugate gradient method combined with the Morozov discrepancy principle. The forward operator is discretized using a spectral approach for the fractional Laplacian and an L1-type scheme adapted to the variable-order Caputo derivative.

The main novelty of the present work lies in the combined treatment of variable-order fractional dynamics and inverse source reconstruction, together with a one-dimensional comparison between constant-order and variable-order models, highlighting the impact of the fractional order on reconstruction accuracy. Furthermore, extensive numerical experiments are conducted for non-smooth source terms, demonstrating the robustness and effectiveness of the proposed approach under different noise levels.

The remainder of the paper is organized as follows. In Section 2, we introduce the mathematical setting and analyze the forward problem. Section 3 is devoted to the formulation and analysis of the inverse problem. In Section 4, we describe the numerical discretization and reconstruction algorithm. Section 5 presents detailed numerical experiments in one and two dimensions. Finally, conclusions are drawn in Section 6.

2. Analysis of the Direct Problem

Let $\Xi \subset \mathbb{R}^d$, $d \geq 1$, be a bounded domain with sufficiently regular boundary, and let $T > 0$ be fixed. We consider the following variable-order time-fractional diffusion equation:

$$\begin{cases} {}^C D_t^{\alpha(t)} u(x,t) + (-\Delta_D)^s u(x,t) = f(x)g(t), & (x,t) \in \Xi \times (0,T), \\ u(x,t) = 0, & x \in \partial\Xi, \quad 0 < t < T, \\ u(x,0) = 0, & x \in \Xi. \end{cases} \tag{2.1}$$

Here $0 < s < 1$, f is a spatial source term, g is a prescribed time-dependent function, and ${}^C D_t^{\alpha(t)}$ denotes the Caputo derivative of variable order.

2.1. **Variable-order Caputo derivative.**

For an absolutely continuous scalar function v, the variable-order Caputo derivative is defined by

$$ {}^C D_t^{\alpha(t)} v(t) = \frac{1}{\Gamma(1-\alpha(t))} \int_0^t (t-\tau)^{-\alpha(t)} v'(\tau)\, d\tau, \qquad 0 < t < T. \tag{2.2}$$

Throughout the paper, we assume

$$0 < \alpha_* \leq \alpha(t) \leq \alpha^* < 1, \qquad \alpha \in C^1([0,T]). \tag{2.3}$$

The condition (2.3) guarantees that the singular memory kernel remains integrable and avoids degeneration at the endpoints $\alpha = 0$ and $\alpha = 1$.

Remark 2.1. *Condition* (2.3) *alone controls only the pointwise range of $\alpha(t)$, not the size of $\alpha'(t)$. As explained in Remark 2.3 below, the energy and comparison arguments used in this paper implicitly require additional control of this type; the precise minimal hypothesis is left open and is stated explicitly as Assumptions 2.1 and 3.2.*

2.2. **Spectral fractional Laplacian.** The spatial operator used in this work is the *spectral fractional Laplacian*. Let $-\Delta_D$ be the classical Dirichlet Laplacian on Ξ. We denote by $\{(\mu_n, \phi_n)\}_{n\geq 1}$ its eigenpairs:

$$-\Delta_D \phi_n = \mu_n \phi_n \quad \text{in } \Xi, \qquad \phi_n = 0 \quad \text{on } \partial\Xi, \tag{2.4}$$

where

$$0 < \mu_1 \leq \mu_2 \leq \cdots, \qquad \mu_n \to \infty, \tag{2.5}$$

and $\{\phi_n\}_{n\geq 1}$ forms an orthonormal basis of $L^2(\Xi)$.

For $0 < s < 1$, the spectral fractional Laplacian is defined by

$$(-\Delta_D)^s v = \sum_{n=1}^{\infty} \mu_n^s v_n \phi_n, \qquad v_n = (v, \phi_n)_{L^2(\Xi)}. \tag{2.6}$$

For simplicity, we set

$$\lambda_n := \mu_n^s. \tag{2.7}$$

Thus,

$$(-\Delta_D)^s \phi_n = \lambda_n \phi_n. \tag{2.8}$$

Remark 2.2. *The operator* (2.6) *is different from the integral fractional Laplacian defined by a hypersingular integral on $\mathbb{R}^d$. In this paper, the theoretical analysis and the numerical experiments are based on the spectral fractional Laplacian. This choice is convenient for both one-dimensional and two-dimensional numerical tests, since the eigenfunctions are explicit on simple domains such as $(0,1)$ and $(0,1)^2$.*

2.3. **Fractional energy space.** We introduce the spectral fractional energy space

$$H_D^s(\Xi) = \left\{ v \in L^2(\Xi) : \sum_{n=1}^{\infty} \lambda_n |v_n|^2 < \infty \right\}, \tag{2.9}$$

where $v_n = (v, \phi_n)_{L^2(\Xi)}$. The space $H_D^s(\Xi)$ is equipped with the norm

$$\|v\|^2_{H_D^s(\Xi)} = \sum_{n=1}^{\infty} (1 + \lambda_n) |v_n|^2. \tag{2.10}$$

The bilinear form associated with $(-\Delta_D)^s$ is

$$a_s(u, v) = \sum_{n=1}^{\infty} \lambda_n u_n v_n, \qquad u, v \in H_D^s(\Xi). \tag{2.11}$$

It is symmetric and continuous:

$$|a_s(u, v)| \leq \|u\|_{H_D^s(\Xi)} \|v\|_{H_D^s(\Xi)}. \tag{2.12}$$

Moreover,

$$a_s(v,v) = \sum_{n=1}^{\infty} \lambda_n |v_n|^2 = \|(-\Delta_D)^{s/2} v\|^2_{L^2(\Xi)}. \tag{2.13}$$

Since $\lambda_1 > 0$, we have the Poincare-type inequality

$$\|v\|^2_{L^2(\Xi)} \le \frac{1}{\lambda_1} a_s(v,v), \qquad v \in H^s_D(\Xi). \tag{2.14}$$

2.4. **Weak formulation.** We assume throughout this section that

$$f \in L^2(\Xi), \qquad g \in L^2(0,T). \tag{2.15}$$

Definition 2.1. *A function u is called a weak solution of* (2.1) *if*

$$u \in L^2(0,T; H^s_D(\Xi)), \qquad {}^C D_t^{\alpha(t)} u \in L^2(0,T; (H^s_D(\Xi))'), \tag{2.16}$$

with $u(\cdot,0) = 0$ in $L^2(\Xi)$, and if

$$\left\langle {}^C D_t^{\alpha(t)} u(t), v \right\rangle_{(H^s_D)', H^s_D} + a_s(u(t), v) = g(t)(f, v)_{L^2(\Xi)} \tag{2.17}$$

for every $v \in H^s_D(\Xi)$ and for almost every $t \in (0,T)$.

2.5. **Galerkin approximation.** For each $m \in \mathbb{N}$, define

$$V_m = \operatorname{span}\{\phi_1, \ldots, \phi_m\}. \tag{2.18}$$

We seek an approximate solution

$$u_m(x,t) = \sum_{j=1}^{m} d_j^m(t) \phi_j(x). \tag{2.19}$$

The Galerkin problem is: find $u_m(t) \in V_m$ such that

$$\left({}^C D_t^{\alpha(t)} u_m(t), \phi_i \right)_{L^2(\Xi)} + a_s(u_m(t), \phi_i) = g(t)(f, \phi_i)_{L^2(\Xi)} \tag{2.20}$$

for $i = 1, \ldots, m$, with $u_m(\cdot,0) = 0$.

Using the orthogonality of $\{\phi_n\}$ and the identity $(-\Delta_D)^s \phi_i = \lambda_i \phi_i$, we obtain

$${}^C D_t^{\alpha(t)} d_i^m(t) + \lambda_i d_i^m(t) = f_i g(t), \qquad d_i^m(0) = 0, \tag{2.21}$$

where

$$f_i = (f, \phi_i)_{L^2(\Xi)}. \tag{2.22}$$

Thus, for fixed m, the Galerkin system consists of m scalar linear variable-order fractional equations. Under (2.3) and (2.15), this finite-dimensional system admits a unique solution. Therefore u_m is well defined.

2.6. **Energy inequality.** We now derive estimates independent of m. Taking $u_m(t)$ as a test function in (2.20), summing over $i = 1, \dots, m$, and using (2.19), we get

$$\left({}^C D_t^{\alpha(t)} u_m(t), u_m(t)\right)_{L^2(\Xi)} + a_s(u_m(t), u_m(t)) = g(t)(f, u_m(t))_{L^2(\Xi)}. \tag{2.23}$$

The remaining energy argument relies on a lower bound for the left-hand term of (2.23) in terms of ${}^C D_t^{\alpha(t)} \|u_m(t)\|^2$. For a *constant* order $\alpha(t) \equiv \alpha$, the elementary inequality

$$\left({}^C D_t^{\alpha} v(t), v(t)\right)_{L^2(\Xi)} \ \geq \ \tfrac{1}{2}\, {}^C D_t^{\alpha} \|v(t)\|^2_{L^2(\Xi)} \tag{2.24}$$

is classical (see, e.g., [16] and [17]) for the constant-order Caputo case). For a *genuinely variable* order $\alpha(t)$, the operator ${}^C D_t^{\alpha(t)}$ no longer has a time-translation-invariant convolution structure, and the proof of (2.24) does not carry over verbatim; in general an additional term depending on $\alpha'(t)$ is expected to appear, and establishing a variable-order analogue of (2.24) (or of the associated comparison / minimum principle used in Section 3.2) is the subject of ongoing research on variable-order fractional operators. We therefore isolate the needed inequality as an explicit standing hypothesis rather than presenting it as an established fact.

Assumption 2.1 (Variable-order energy inequality)**.** *For every $v \in H^1(0, T; L^2(\Xi))$ with $v(\cdot, 0) = 0$,*

$$\left({}^C D_t^{\alpha(t)} v(t), v(t)\right)_{L^2(\Xi)} \ \geq \ \tfrac{1}{2}\, {}^C D_t^{\alpha(t)} \|v(t)\|^2_{L^2(\Xi)} \qquad \textit{for a.e. } t \in (0, T). \tag{2.25}$$

Remark 2.3. *Assumption 2.1 holds when $\alpha(t) \equiv \alpha$ is constant. For a genuinely variable order it is known to hold under additional structural conditions on $\alpha(\cdot)$ beyond* (2.3) *(see the discussion of "corrected" discrete energy inequalities for variable-order Caputo operators in the recent literature on variable-order time-fractional PDEs). All well-posedness results in this section (Theorem 2.1) should accordingly be read as conditional on Assumption 2.1; they apply unconditionally in the constant-order case $\alpha(t) \equiv \alpha$, which is also the case used for the "constant-order" numerical comparison in Section 5.*

If $v = u_m(t) = \sum_{j=1}^m d_j^m(t)\phi_j$, Assumption 2.1 applied componentwise gives

$$\left({}^C D_t^{\alpha(t)} u_m(t), u_m(t)\right)_{L^2(\Xi)} = \sum_{j=1}^{m} {}^C D_t^{\alpha(t)} d_j^m(t)\, d_j^m(t) \ \geq \ \tfrac{1}{2} {}^C D_t^{\alpha(t)} \|u_m(t)\|^2_{L^2(\Xi)}, \tag{2.26}$$

which is (2.25) for u_m.

Using Cauchy's inequality and (2.14), the right-hand side of (2.23) satisfies

$$\begin{aligned} |g(t)(f, u_m(t))_{L^2(\Xi)}| &\leq |g(t)| \|f\|_{L^2(\Xi)} \|u_m(t)\|_{L^2(\Xi)} \\ &\leq \frac{1}{2\lambda_1} |g(t)|^2 \|f\|^2_{L^2(\Xi)} + \frac{\lambda_1}{2} \|u_m(t)\|^2_{L^2(\Xi)} \\ &\leq C|g(t)|^2 \|f\|^2_{L^2(\Xi)} + \frac{1}{2} a_s(u_m(t), u_m(t)). \end{aligned} \tag{2.27}$$

Substituting Assumption 2.1 and (2.27) into (2.23), we obtain, under Assumption 2.1,

$$\frac{1}{2} {}^C D_t^{\alpha(t)} \|u_m(t)\|^2_{L^2(\Xi)} + \frac{1}{2} a_s(u_m(t), u_m(t)) \leq C|g(t)|^2 \|f\|^2_{L^2(\Xi)}. \tag{2.28}$$

Integrating over $(0, T)$ and using the bounds on $\alpha(t)$, we obtain

$$\|u_m\|_{L^2(0,T;H^s_D(\Xi))} \leq C\|f\|_{L^2(\Xi)}\|g\|_{L^2(0,T)}, \tag{2.29}$$

where $C > 0$ is independent of m.

Moreover, from the Galerkin equation,

$${}^C D_t^{\alpha(t)} u_m = -(-\Delta_D)^s u_m + P_m f\, g(t), \tag{2.30}$$

where P_m is the L^2-orthogonal projection onto V_m. Hence,

$$\begin{aligned} \|{}^C D_t^{\alpha(t)} u_m\|_{L^2(0,T;(H^s_D)')} &\leq \|(-\Delta_D)^s u_m\|_{L^2(0,T;(H^s_D)')} + \|P_m f\, g\|_{L^2(0,T;(H^s_D)')} \\ &\leq C\|u_m\|_{L^2(0,T;H^s_D(\Xi))} + C\|f\|_{L^2(\Xi)}\|g\|_{L^2(0,T)}. \end{aligned} \tag{2.31}$$

Using (2.29), we get

$$\|{}^C D_t^{\alpha(t)} u_m\|_{L^2(0,T;(H^s_D)')} \leq C\|f\|_{L^2(\Xi)}\|g\|_{L^2(0,T)}. \tag{2.32}$$

2.7. **Existence of weak solutions.** From (2.29) and (2.32), the sequence $\{u_m\}$ is bounded in $L^2(0, T; H^s_D(\Xi))$, while $\{{}^C D_t^{\alpha(t)} u_m\}$ is bounded in $L^2(0, T; (H^s_D(\Xi))')$. Therefore, there exist a subsequence, still denoted by $\{u_m\}$, and a function u such that

$$u_m \rightharpoonup u \quad \text{weakly in } L^2(0, T; H^s_D(\Xi)), \tag{2.33}$$

and

$${}^C D_t^{\alpha(t)} u_m \rightharpoonup {}^C D_t^{\alpha(t)} u \quad \text{weakly in } L^2(0, T; (H^s_D(\Xi))'). \tag{2.34}$$

Let $v \in H^s_D(\Xi)$ be fixed and let $P_m v$ be its projection onto V_m. Since $P_m v \to v$ strongly in $H^s_D(\Xi)$, we may pass to the limit in

$$\left\langle {}^C D_t^{\alpha(t)} u_m(t), P_m v \right\rangle + a_s(u_m(t), P_m v) = g(t)(f, P_m v)_{L^2(\Xi)}. \tag{2.35}$$

Using (2.33) and (2.34), we obtain

$$\left\langle {}^C D_t^{\alpha(t)} u(t), v \right\rangle + a_s(u(t), v) = g(t)(f, v)_{L^2(\Xi)}. \tag{2.36}$$

Thus u satisfies the weak formulation (2.17). Therefore, a weak solution exists (under Assumption 2.1, which was used to derive the m-independent bounds (2.29)–(2.32)).

2.8. **Uniqueness.** Assume that u_1 and u_2 are two weak solutions corresponding to the same source f. Set

$$w = u_1 - u_2.$$

Then w satisfies

$${}^C D_t^{\alpha(t)} w + (-\Delta_D)^s w = 0, \qquad w(\cdot, 0) = 0. \tag{2.37}$$

Testing (2.37) by $w(t)$ gives

$$\left({}^C D_t^{\alpha(t)} w(t), w(t)\right)_{L^2(\Xi)} + a_s(w(t), w(t)) = 0. \tag{2.38}$$

Using Assumption 2.1, we obtain

$$\frac{1}{2} {}^C D_t^{\alpha(t)} \|w(t)\|^2_{L^2(\Xi)} + a_s(w(t), w(t)) \le 0. \tag{2.39}$$

Since $a_s(w, w) \ge 0$ and $w(\cdot, 0) = 0$, it follows that

$$\|w(t)\|^2_{L^2(\Xi)} = 0 \qquad \text{for all } 0 \le t \le T.$$

Hence $u_1 = u_2$. Therefore, under Assumption 2.1, the weak solution is unique.

2.9. **Continuous dependence on the source.** Let $f_1, f_2 \in L^2(\Xi)$ and let u_1, u_2 be the corresponding weak solutions. Set

$$z = u_1 - u_2, \qquad F = f_1 - f_2.$$

Then

$${}^C D_t^{\alpha(t)} z + (-\Delta_D)^s z = F(x)g(t), \qquad z(\cdot, 0) = 0. \tag{2.40}$$

Repeating the same energy argument used above (again under Assumption 2.1) gives

$$\|z\|_{L^2(0,T;H^s_D(\Xi))} \le C\|F\|_{L^2(\Xi)}\|g\|_{L^2(0,T)}. \tag{2.41}$$

Therefore,

$$\|u_1 - u_2\|_{L^2(0,T;H^s_D(\Xi))} \le C\|f_1 - f_2\|_{L^2(\Xi)}\|g\|_{L^2(0,T)}. \tag{2.42}$$

Theorem 2.1 (Well-posedness of the direct problem, conditional on Assumption 2.1)**.** *Assume that $\Xi \subset \mathbb{R}^d$ is bounded, $0 < s < 1$, that* (2.3) *and* (2.15) *hold, and that Assumption 2.1 holds. Then the direct problem* (2.1) *admits a unique weak solution*

$$u \in L^2(0, T; H^s_D(\Xi)), \qquad {}^C D_t^{\alpha(t)} u \in L^2(0, T; (H^s_D(\Xi))').$$

Moreover, the estimate

$$\|u\|_{L^2(0,T;H^s_D(\Xi))} + \|{}^C D_t^{\alpha(t)} u\|_{L^2(0,T;(H^s_D(\Xi))')} \le C\|f\|_{L^2(\Xi)}\|g\|_{L^2(0,T)} \tag{2.43}$$

holds, where $C > 0$ is independent of f. In particular, all conclusions of this theorem hold unconditionally when $\alpha(t) \equiv \alpha$ is constant.

Remark 2.4. *The above theorem shows that the forward map*

$$f \mapsto u(\cdot, T)$$

is well defined from $L^2(\Xi)$ into $L^2(\Xi)$, conditional on Assumption 2.1. This property will be used in the next section to formulate and analyze the inverse source problem from terminal-time measurements.

3. The Inverse Source Problem

In this section, we formulate the inverse source problem associated with (2.1). The unknown quantity is the spatial factor $f(x)$ in the separable source term $f(x)g(t)$, while the time-dependent factor $g(t)$ is assumed to be known.

Let u_f denote the weak solution corresponding to a given source $f \in L^2(\Xi)$. The available measurement is the terminal-time observation

$$u_f(\cdot, T) = h^\delta \quad \text{in } L^2(\Xi), \tag{3.1}$$

where h^δ denotes noisy data satisfying

$$\|h^\delta - h\|_{L^2(\Xi)} \leq \delta, \qquad h = u_f(\cdot, T). \tag{3.2}$$

The inverse problem is therefore stated as follows:

> Given the terminal observation h^δ, determine the unknown spatial source $f \in L^2(\Xi)$ in the variable-order space-fractional diffusion equation (2.1).

We define the parameter-to-observation operator

$$\mathcal{K} : L^2(\Xi) \longrightarrow L^2(\Xi), \qquad \mathcal{K}f = u_f(\cdot, T). \tag{3.3}$$

By the linearity of the direct problem with respect to f, the operator $\mathcal{K}$ is linear. Moreover, from the continuous dependence estimate (2.41), there exists a constant $C > 0$ such that

$$\|\mathcal{K}f\|_{L^2(\Xi)} \leq C\|f\|_{L^2(\Xi)}\|g\|_{L^2(0,T)}. \tag{3.4}$$

Hence $\mathcal{K}$ is a bounded linear operator from $L^2(\Xi)$ into $L^2(\Xi)$.

3.1. **Spectral representation of the forward map.** We now derive a modal representation of the forward map. Let $\{\phi_n\}_{n\geq 1}$ be the orthonormal eigenbasis of the Dirichlet Laplacian introduced in (2.4). Expanding

$$f(x) = \sum_{n=1}^{\infty} f_n \phi_n(x), \qquad u_f(x,t) = \sum_{n=1}^{\infty} u_n(t)\phi_n(x), \tag{3.5}$$

with

$$f_n = (f, \phi_n)_{L^2(\Xi)}, \qquad u_n(t) = (u_f(\cdot, t), \phi_n)_{L^2(\Xi)},$$

and using

$$(-\Delta_D)^s \phi_n = \lambda_n \phi_n, \qquad \lambda_n = \mu_n^s,$$

we obtain, for each $n \geq 1$,

$${}^C D_t^{\alpha(t)} u_n(t) + \lambda_n u_n(t) = f_n g(t), \qquad u_n(0) = 0. \tag{3.6}$$

For each $n \geq 1$, let Θ_n be the solution of the auxiliary problem

$${}^C D_t^{\alpha(t)} \Theta_n(t) + \lambda_n \Theta_n(t) = g(t), \qquad \Theta_n(0) = 0. \tag{3.7}$$

By linearity, the solution of (3.6) is

$$u_n(t) = f_n \Theta_n(t). \tag{3.8}$$

Evaluating at $t = T$ gives

$$u_n(T) = f_n\Theta_n(T). \tag{3.9}$$

Consequently,

$$\mathcal{K}f = \sum_{n=1}^{\infty} \Theta_n(T) f_n \phi_n. \tag{3.10}$$

Thus, with respect to the spectral basis, the forward operator is diagonal, self-adjoint, and its eigenvalues (singular values, once Assumption 3.2 below guarantees they are positive) are given by

$$\sigma_n = \Theta_n(T).$$

Remark 3.1. *When $\alpha(t) \equiv \alpha$ is constant, the coefficients Θ_n can be expressed using Mittag–Leffler functions, and their strict positivity $\Theta_n(T) > 0$ is a classical consequence of the strong maximum principle for constant-order subdiffusion equations. For a genuinely variable order $\alpha(t)$, such a closed representation is generally not available, and the positivity of $\Theta_n(T)$ is correspondingly not automatic; we isolate it as Assumption 3.2 below. Given that assumption, the diagonal relation* (3.9) *is enough to prove uniqueness and to explain the ill-posedness of the inverse problem.*

3.2. **Identifiability of the source.** To prove uniqueness, we impose a mild positivity assumption on the temporal factor.

Assumption 3.1. *The function g satisfies*

$$g(t) \geq 0 \quad \text{for a.e. } t \in (0, T), \qquad g \not\equiv 0. \tag{3.11}$$

We next isolate, as an explicit hypothesis, the positivity property of $\Theta_n(T)$ that drives all identifiability and stability results below.

Assumption 3.2 (Strict positivity of the modal response)**.** *For every $n \geq 1$, the solution Θ_n of* (3.7) *satisfies $\Theta_n(t) \geq 0$ on $[0, T]$ and*

$$\Theta_n(T) > 0. \tag{3.12}$$

Remark 3.2. *When $\alpha(t) \equiv \alpha$ is constant, Assumption 3.2 is a theorem: it follows from the strong maximum principle for constant-order Caputo subdiffusion equations (see, e.g., [18] for the weak maximum principle, and [19] for the strict version), applied together with a variation-of-constants representation of Θ_n through a Mittag–Leffler resolvent kernel, which is known to be positive. For a genuinely variable order $\alpha(t)$, a minimum principle for the Caputo derivative evaluated pointwise as ${}^C D_t^{\alpha(t_0)} \Theta_n(t_0)$ at a minimizer t_0, together with the existence and positivity of an analogous resolvent kernel $G_n(T, \tau)$, are not automatic consequences of* (2.3)*; comparison principles of this type for variable-order Caputo derivatives have only recently begun to be established in the literature, typically under extra structural hypotheses on $\alpha(\cdot)$. We therefore state Assumption 3.2 explicitly rather than present it as a consequence of* (2.3) *alone. All of Theorem 3.1, Proposition 3.1, and Theorem 3.2 below should be read as conditional on Assumption 3.2; as in Section 2.6, they hold unconditionally in the constant-order case.*

Theorem 3.1 (Identifiability, conditional on Assumption 3.2)**.** *Assume that* (2.3), (2.15), (3.11), *and Assumption 3.2 hold. Let* $f_1, f_2 \in L^2(\Xi)$ *and let* u_1, u_2 *be the corresponding weak solutions of* (2.1). *If*

$$u_1(\cdot, T) = u_2(\cdot, T) \qquad \text{in } L^2(\Xi), \tag{3.13}$$

then

$$f_1 = f_2 \qquad \text{in } L^2(\Xi). \tag{3.14}$$

Proof. Set

$$w = u_1 - u_2, \qquad F = f_1 - f_2.$$

Then w solves

$${}^C D_t^{\alpha(t)} w + (-\Delta_D)^s w = F(x) g(t), \qquad w(\cdot, 0) = 0. \tag{3.15}$$

Expand

$$F(x) = \sum_{n=1}^{\infty} F_n \phi_n(x), \qquad w(x,t) = \sum_{n=1}^{\infty} w_n(t) \phi_n(x).$$

For each $n \geq 1$, the coefficient w_n satisfies

$${}^C D_t^{\alpha(t)} w_n(t) + \lambda_n w_n(t) = F_n g(t), \qquad w_n(0) = 0.$$

Using the definition of Θ_n, we obtain

$$w_n(t) = F_n \Theta_n(t).$$

At $t = T$, this gives

$$w_n(T) = F_n \Theta_n(T). \tag{3.16}$$

The assumption $u_1(\cdot, T) = u_2(\cdot, T)$ implies $w(\cdot, T) = 0$ in $L^2(\Xi)$. Therefore,

$$w_n(T) = (w(\cdot, T), \phi_n)_{L^2(\Xi)} = 0 \qquad \forall n \geq 1.$$

From (3.16),

$$F_n \Theta_n(T) = 0 \qquad \forall n \geq 1.$$

By Assumption 3.2, $\Theta_n(T) > 0$ for all n. Hence

$$F_n = 0 \qquad \forall n \geq 1.$$

Since $\{\phi_n\}_{n \geq 1}$ is complete in $L^2(\Xi)$, it follows that

$$F = 0 \quad \text{in } L^2(\Xi).$$

Thus $f_1 = f_2$ in $L^2(\Xi)$. □

3.3. **Ill-posedness.** Although the source is uniquely determined by the terminal observation (under Assumption 3.2), the reconstruction is unstable. Indeed, from (3.9), the formal inversion formula is

$$f_n = \frac{h_n}{\Theta_n(T)}, \qquad h_n = (h, \phi_n)_{L^2(\Xi)}. \tag{3.17}$$

Since the forward diffusion process smooths high-frequency modes, the coefficients $\Theta_n(T)$ are expected to decay to zero as $n \to \infty$; in the constant-order case this decay follows from the explicit Mittag–Leffler representation of Θ_n, while for a genuinely variable order it is consistent with, but not separately proved from, Assumption 3.2 alone. We record the ill-posedness conclusion under the explicit hypothesis that this decay occurs.

Assumption 3.3 (Modal decay). $\Theta_n(T) \to 0$ *as* $n \to \infty$.

Proposition 3.1. *Under Assumptions 3.2 and 3.3, the inverse source problem is ill-posed in the sense of Hadamard.*

Proof. It is enough to show that the inverse map is not continuous. Let $\{e_n\}$ be the spectral basis, with $e_n = \phi_n$, and consider a sequence of perturbations in the data of the form

$$h^{(n)} = \varepsilon_n \phi_n,$$

where $\varepsilon_n > 0$ and $\varepsilon_n \to 0$. Then

$$\|h^{(n)}\|_{L^2(\Xi)} = \varepsilon_n \to 0.$$

The corresponding source obtained from the formal inverse relation is

$$f^{(n)} = \frac{\varepsilon_n}{\Theta_n(T)} \phi_n.$$

Therefore,

$$\|f^{(n)}\|_{L^2(\Xi)} = \frac{\varepsilon_n}{|\Theta_n(T)|}.$$

Since $|\Theta_n(T)| \to 0$ by Assumption 3.3, we can choose ε_n such that

$$\varepsilon_n \to 0, \qquad \frac{\varepsilon_n}{|\Theta_n(T)|} \to \infty.$$

For instance, take

$$\varepsilon_n = \sqrt{|\Theta_n(T)|}.$$

Then $\varepsilon_n \to 0$, while

$$\|f^{(n)}\|_{L^2(\Xi)} = \frac{1}{\sqrt{|\Theta_n(T)|}} \to \infty.$$

Thus arbitrarily small perturbations in the terminal data may produce arbitrarily large deviations in the reconstructed source. Hence the inverse problem is ill-posed. □

3.4. **Finite-dimensional conditional stability.** Although global Lipschitz stability cannot be expected in the whole space $L^2(\Xi)$, a Lipschitz estimate can be obtained on finite-dimensional admissible sets. Let

$$\mathcal{A}_N = \mathrm{span}\{\phi_1, \dots, \phi_N\}. \tag{3.18}$$

Theorem 3.2 (Conditional stability, conditional on Assumption 3.2)**.** *Let $N \in \mathbb{N}$ be fixed. Assume that $f_1, f_2 \in \mathcal{A}_N$, and let u_1, u_2 be the corresponding weak solutions. Under Assumption 3.2, there exists a constant $C_N > 0$ such that*

$$\|f_1 - f_2\|_{L^2(\Xi)} \le C_N \|u_1(\cdot, T) - u_2(\cdot, T)\|_{L^2(\Xi)}. \tag{3.19}$$

Proof. Let

$$F = f_1 - f_2, \qquad w = u_1 - u_2.$$

Since $f_1, f_2 \in \mathcal{A}_N$, we have

$$F = \sum_{n=1}^{N} F_n \phi_n.$$

As before,

$$w_n(T) = F_n \Theta_n(T), \qquad n = 1, \dots, N.$$

Therefore,

$$F_n = \frac{w_n(T)}{\Theta_n(T)}.$$

Using Parseval's identity,

$$\|F\|^2_{L^2(\Xi)} = \sum_{n=1}^{N} |F_n|^2 = \sum_{n=1}^{N} \frac{|w_n(T)|^2}{|\Theta_n(T)|^2}.$$

Let

$$m_N = \min_{1 \le n \le N} |\Theta_n(T)|.$$

By Assumption 3.2 (applied to the finitely many indices $n = 1, \dots, N$), $m_N > 0$. Hence

$$\|F\|^2_{L^2(\Xi)} \le \frac{1}{m_N^2} \sum_{n=1}^{N} |w_n(T)|^2.$$

Since

$$\sum_{n=1}^{N} |w_n(T)|^2 \le \|w(\cdot, T)\|^2_{L^2(\Xi)},$$

we obtain

$$\|F\|_{L^2(\Xi)} \le \frac{1}{m_N} \|w(\cdot, T)\|_{L^2(\Xi)}.$$

Thus (3.19) holds with

$$C_N = \frac{1}{m_N}.$$

□

4. Regularization and Numerical Reconstruction

Due to the ill-posedness established in the previous section, direct inversion of the operator equation

$$\mathcal{K}f = h^{\delta} \tag{4.1}$$

is unstable. Therefore, regularization techniques are required.

4.1. Tikhonov regularization.

We consider the classical Tikhonov functional

$$J_{\beta}(f) = \|\mathcal{K}f - h^{\delta}\|^2_{L^2(\Xi)} + \beta\|f\|^2_{L^2(\Xi)}, \qquad \beta > 0. \tag{4.2}$$

Proposition 4.1. *For every $\beta > 0$, the minimization problem*

$$\min_{f\in L^2(\Xi)} J_{\beta}(f)$$

admits a unique solution $f_{\beta} \in L^2(\Xi)$.

Proof. The functional J_{β} is strictly convex, continuous, and coercive since

$$J_{\beta}(f) \geq \beta\|f\|^2_{L^2(\Xi)}.$$

Hence, the existence and uniqueness of the minimizer follow from standard convex analysis arguments in Hilbert spaces. □

The minimizer satisfies the normal equation

$$(\mathcal{K}^*\mathcal{K} + \beta I)f_{\beta} = \mathcal{K}^*h^{\delta}. \tag{4.3}$$

4.2. Stability estimate.

The classical two-term Tikhonov convergence rate requires, in addition to the noise bound (3.2), a *source condition* on the exact solution $f^{\dagger}$; we state it explicitly since it was implicit (and unused) in the original derivation.

Assumption 4.1 (Source condition)**.** *There exists $\omega \in L^2(\Xi)$, with $\|\omega\|_{L^2(\Xi)} \leq \rho$, such that*

$$f^{\dagger} = \mathcal{K}^*\omega = \mathcal{K}\omega,$$

where the last equality uses the self-adjointness of $\mathcal{K}$ established in (3.10)*.*

Theorem 4.1. *Let $f^{\dagger}$ be the exact solution corresponding to exact data h, satisfying Assumption 4.1 with constant ρ, and let f_{β} be the minimizer of* (4.2) *with noisy data h^{δ} satisfying* (3.2)*. Then*

$$\|f_{\beta} - f^{\dagger}\|_{L^2(\Xi)} \leq \frac{\delta}{2\sqrt{\beta}} + \frac{\rho}{2}\sqrt{\beta}, \tag{4.4}$$

in particular $\|f_{\beta} - f^{\dagger}\|_{L^2(\Xi)} \leq C(\delta/\sqrt{\beta} + \sqrt{\beta})$ with $C = \max(1/2, \rho/2)$.

Proof. Subtracting the normal equations for f_β and $f^\dagger$ yields

$$(\mathcal{K}^*\mathcal{K} + \beta I)(f_\beta - f^\dagger) = \mathcal{K}^*(h^\delta - h) - \beta f^\dagger.$$

By (3.10), $\mathcal{K}$ is diagonal and self-adjoint in the eigenbasis $\{\phi_n\}$ with real eigenvalues $\sigma_n = \Theta_n(T)$, so $\mathcal{K}^* = \mathcal{K}$ and the above identity decouples modewise:

$$(\sigma_n^2 + \beta)\,(f_\beta - f^\dagger)_n = \sigma_n\,(h^\delta - h)_n - \beta f_n^\dagger, \qquad n \geq 1.$$

For the noise term, the elementary bound $\sigma_n/(\sigma_n^2+\beta) \leq 1/(2\sqrt{\beta})$ (AM–GM inequality) gives

$$\left\| \sum_n \frac{\sigma_n}{\sigma_n^2+\beta}(h^\delta - h)_n \phi_n \right\|_{L^2(\Xi)} \leq \frac{1}{2\sqrt{\beta}}\, \|h^\delta - h\|_{L^2(\Xi)} \leq \frac{\delta}{2\sqrt{\beta}}.$$

For the bias term, using Assumption 4.1 ($f_n^\dagger = \sigma_n \omega_n$) and again $\sigma_n^2/(\sigma_n^2+\beta) \leq 1$ together with $\beta\sigma_n/(\sigma_n^2+\beta) \leq \sqrt{\beta}/2$,

$$\left\| \sum_n \frac{\beta}{\sigma_n^2+\beta} f_n^\dagger \phi_n \right\|_{L^2(\Xi)} = \left\| \sum_n \frac{\beta\sigma_n}{\sigma_n^2+\beta} \omega_n \phi_n \right\|_{L^2(\Xi)} \leq \frac{\sqrt{\beta}}{2}\, \|\omega\|_{L^2(\Xi)} \leq \frac{\sqrt{\beta}}{2}\,\rho.$$

Combining the two estimates via the triangle inequality gives (4.4). □

Remark 4.1. *Without Assumption 4.1, only the weaker bound $\|f_\beta - f^\dagger\|_{L^2(\Xi)} \leq \delta/(2\sqrt{\beta}) + \|f^\dagger\|_{L^2(\Xi)}$ is available from the same computation (taking the crude bound $\beta/(\sigma_n^2+\beta) \leq 1$ instead), which does not vanish as $\beta \to 0$; convergence $f_\beta \to f^\dagger$ as $(\delta, \beta) \to (0,0)$ with $\delta^2/\beta \to 0$ still holds by the standard (rate-free) Tikhonov theory, but without the explicit $O(\sqrt{\beta})$ rate.*

4.3. **Iterative regularization via CGM.** Instead of solving (4.3) directly, we employ an iterative regularization method based on the Conjugate Gradient Method (CGM).

We consider the least-squares functional

$$J(f) = \frac{1}{2}\|\mathcal{K}f - h^\delta\|_{L^2(\Xi)}^2. \tag{4.5}$$

Its gradient is given by

$$\nabla J(f) = \mathcal{K}^*(\mathcal{K}f - h^\delta). \tag{4.6}$$

Starting from an initial guess $f^0 = 0$, the CGM iteration reads:

$$r^k = \mathcal{K}f^k - h^\delta, \tag{4.7}$$

$$g^k = \mathcal{K}^* r^k, \tag{4.8}$$

$$d^k = -g^k + \beta_k d^{k-1}, \tag{4.9}$$

$$f^{k+1} = f^k + \alpha_k d^k, \tag{4.10}$$

where

$$\alpha_k = -\frac{\langle r^k, \mathcal{K}d^k\rangle}{\|\mathcal{K}d^k\|^2}, \tag{4.11}$$

and

$$\beta_k = \frac{\|g^k\|^2}{\|g^{k-1}\|^2}. \tag{4.12}$$

4.4. **Morozov discrepancy principle.** To stabilize the iteration, we adopt Morozov's discrepancy principle.

Definition 4.1. *Let $\tau > 1$. The iteration is stopped at the first index k^* such that*

$$\|\mathcal{K} f^{k^*} - h^\delta\| \leq \tau\delta. \tag{4.13}$$

Remark 4.2. *The discrepancy principle prevents overfitting to noisy data and provides an implicit regularization effect. In practice, the stopping index k^* decreases as the noise level δ increases.*

4.5. **Convergence result.**

Theorem 4.2. *Assume that $\mathcal{K}$ is compact, injective, and has dense range in $L^2(\Xi)$ (equivalently, by* (3.10)*, that $\Theta_n(T) \neq 0$ for every n). Let f^{k^*} be the CGM iterate obtained using Morozov's principle with $\tau > 1$ fixed. Then*

$$f^{k^*} \to f^\dagger \quad \text{in } L^2(\Xi) \quad \text{as } \delta \to 0,$$

where $f^\dagger$ denotes the (assumed to exist) minimum-norm solution of $\mathcal{K} f = h$.

Proof. This is the classical convergence result for the conjugate gradient method for normal equations (CGNE) combined with Morozov's discrepancy principle applied to a compact, injective operator with dense range; see, e.g., [20] for a full proof. We only note here that compactness of $\mathcal{K}$ implies that the inverse problem is ill-posed (consistently with Proposition 3.1), and that the discrepancy principle (4.13) guarantees that the iteration is terminated at a finite $k^* = k^*(\delta)$ before the noise is amplified, with $k^*(\delta) \to \infty$ as $\delta \to 0$; both facts are used in the cited convergence proof. □

5. Numerical Experiments

In this section, we present numerical experiments to validate the proposed reconstruction method. The goal is to recover an unknown spatial source term from final-time observations of the solution.

All computations are performed using MATLAB. The spatial fractional Laplacian is discretized using a spectral approach, while the time-fractional derivative is approximated using the L1 scheme. The inverse problem is solved by the conjugate gradient method (CGM) combined with Morozov's discrepancy principle. The noisy observation is defined as

$$h^\delta = h(x) + \epsilon\, h(x)\left(2\,\mathrm{rand}(\mathrm{size}(h)) - 1\right),$$

where $\epsilon > 0$ denotes a prescribed relative noise level, and, unless noted otherwise, the discrepancy-principle safety factor in (4.13) is set to $\tau = 1.01$. The magnitude of the noise is quantified by

$$\delta = \|h^\delta - h\|_{L^2(\Omega)}. \tag{5.1}$$

To evaluate the accuracy of the reconstruction, we consider the $L^2(\Omega)$-error defined by

$$E_k = \|f^k - f_{\text{exact}}\|_{L^2(\Omega)}, \tag{5.2}$$

5.1. **One-dimensional case.** We first consider the one-dimensional domain

$$\Xi = (0,1), \qquad T = 1, s = 0.7$$

The temporal function is chosen as

$$g(t) = 1 + t.$$

We compare two models:

- Variable-order model:

$$\alpha(t) = 0.65 + 0.15 \sin(\pi t),$$

- Constant-order model:

$$\alpha(t) \equiv 0.70.$$

The exact source is the nonsmooth function

$$f^1_{\text{exact}}(x) = 1 - |2x - 1|.$$

This example is particularly relevant because the nonsmooth structure introduces high-frequency components that are difficult to reconstruct in inverse problems. We stress that only a single, mild-amplitude variable-order profile ($\alpha(t) \in [0.5, 0.8]$) is tested against a single constant order; the conclusion drawn below on the secondary role of order variability should be read as specific to this configuration rather than as a general statement (see also the remark at the end of Section 5.2).

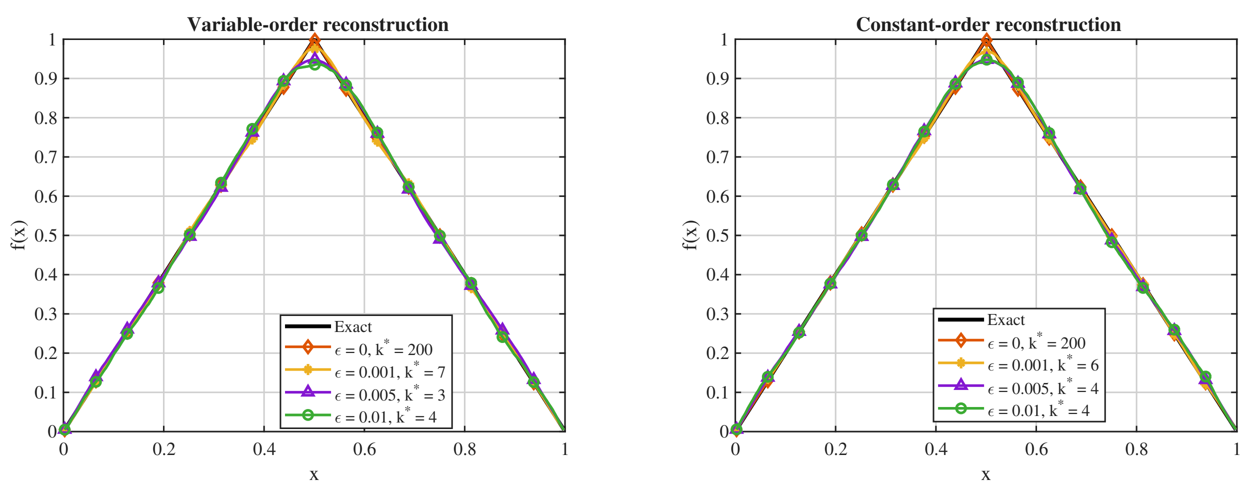

(a) Reconstruction using the variable-order model. (b) Reconstruction using the constant-order model.

FIGURE 1. The numerical results for f^1_{exact} with various noise levels

From these results, several observations can be made.

Table 1. Relative errors and stopping indices in 1D.

Noise ε	Model	k^*	Relative error
0	Variable	200	4.8555×10^{-5}
0	Constant	200	4.8524×10^{-5}
10^{-3}	Variable	7	8.3752×10^{-3}
10^{-3}	Constant	6	8.9479×10^{-3}
5×10^{-3}	Variable	3	1.9468×10^{-2}
5×10^{-3}	Constant	4	1.9318×10^{-2}
10^{-2}	Variable	4	2.2499×10^{-2}
10^{-2}	Constant	4	2.1160×10^{-2}

First, in the noise-free case, both models converge to highly accurate solutions with relative errors of order 10^{-5}. The stopping index reaches the maximum allowed value, indicating that no early stopping is triggered when $\delta = 0$.

Second, as the noise level increases, the stopping index decreases significantly. This reflects the role of Morozov's discrepancy principle as a regularization strategy, preventing overfitting of noisy data.

Third, the reconstruction error increases with the noise level, which confirms the ill-posed nature of the inverse source problem.

Finally, the difference between the variable-order and constant-order models is relatively small in this configuration. For low noise, the variable-order model performs slightly better, while for higher noise levels, both models provide comparable accuracy. This suggests that, *for the mild-amplitude profile $\alpha(t)$ tested here*, the dominant factor in reconstruction quality is the noise, rather than the variation of the fractional order; we do not claim this conclusion extends to variable-order profiles with larger amplitude or higher frequency.

5.2. **Two-dimensional case.** We now consider the two-dimensional domain

$$\Xi = (0,1)^2.$$

The reconstruction below uses the variable-order model $\alpha(t) = 0.65 + 0.15\sin(\pi t)$, $s = 0.7$, with the same $g(t) = 1 + t$ as in the one-dimensional case. Unlike Section 5.1, this experiment does not include a constant-order comparison; a two-dimensional variable-versus-constant-order comparison analogous to Table 1 is left for future work.

The exact source is chosen as a nonsmooth piecewise function:

$$f^2_{exact}(x,y) = \begin{cases} 2, & (x,y) \in [0.4, 0.6]^2, \\ 1, & (x,y) \in [0.25, 0.75]^2 \setminus [0.4, 0.6]^2, \\ 0, & \text{otherwise.} \end{cases}$$

This example contains discontinuities and sharp transitions, making it a challenging benchmark for reconstruction.

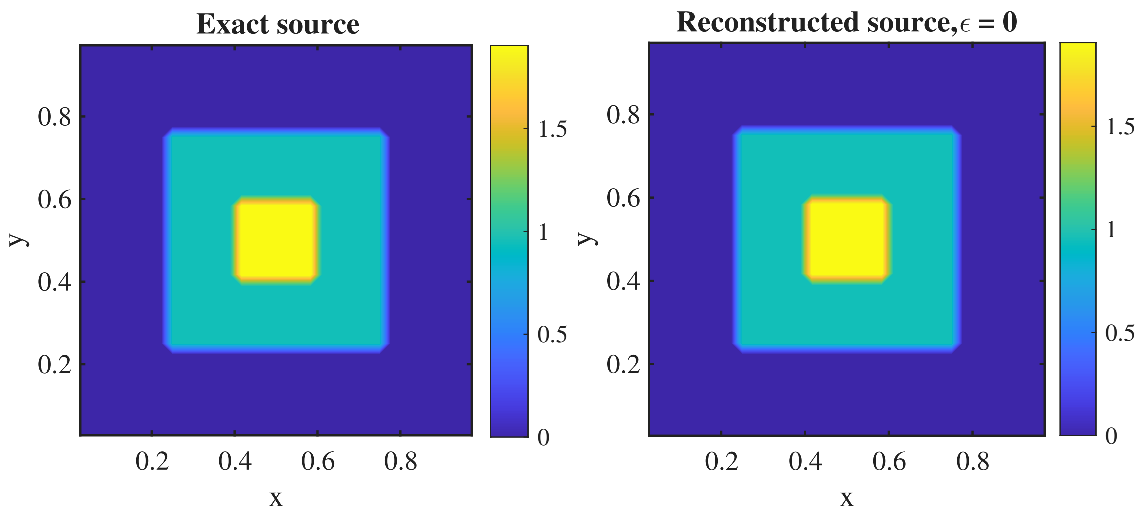

FIGURE 2. Exact source and reconstruction for f^2_{exact} with $\varepsilon = 0$.

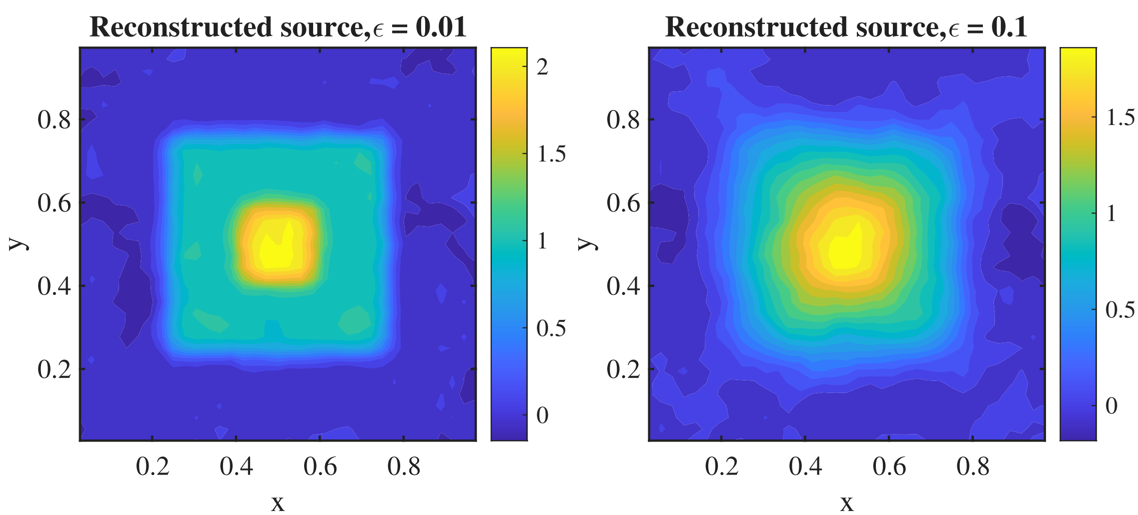

FIGURE 3. Reconstruction for f^2_{exact} with $\varepsilon = 10^{-2}$ and $\varepsilon = 10^{-1}$.

The two-dimensional results are qualitatively consistent with the one-dimensional case, while highlighting additional spatial effects; since no constant-order run was performed in 2D (see above), this consistency is reported only qualitatively and is not the outcome of a direct 1D-style comparison.

In the absence of noise, the reconstructed source matches the exact solution very closely. The plateau structure and the sharp central peak are accurately captured.

When noise is introduced, the reconstruction remains stable. The overall shape of the source is preserved, although some smoothing appears near the discontinuities. This is expected, as the inversion process acts as a low-pass filter, attenuating high-frequency components.

As the noise level increases, the reconstructed solution becomes progressively smoother. However, the main geometric features of the source are still clearly visible. This demonstrates the robustness of the method in higher dimensions.

The surface plot provides additional insight into the reconstruction quality. It shows that the amplitude and location of the maximum are well preserved, even for relatively large noise levels.

Overall, the two-dimensional experiment confirms that the proposed method is capable of accurately reconstructing nonsmooth sources in both low and moderate noise regimes.

5.3. **Discussion.** The numerical experiments demonstrate that the proposed reconstruction framework is effective for both one-dimensional and two-dimensional inverse source problems involving space-time fractional diffusion equations.

The CGM combined with Morozov's discrepancy principle provides stable reconstructions and automatically adapts the stopping iteration to the noise level.

The comparison between variable-order and constant-order models, carried out in the one-dimensional setting, indicates that the influence of the fractional order on reconstruction quality is relatively limited in the tested configuration. Instead, the dominant factor is the noise level and the regularity of the source. As noted above, this comparison was not repeated in two dimensions and was only tested for a single, mild-amplitude variable-order profile, so it should not yet be read as a general conclusion about variable-order effects.

Finally, the results confirm that the proposed approach can handle nonsmooth sources and remains robust in the presence of noise, making it suitable for practical applications involving fractional diffusion models.

6. Conclusion

In this work, we have studied an inverse source problem for a space–time fractional diffusion equation involving a spectral fractional Laplacian in space and a variable-order Caputo derivative in time. The objective was to reconstruct an unknown spatial source term from terminal-time observations, a setting that is particularly challenging due to the strong smoothing effect of the forward operator.

From a theoretical perspective, we analyzed the associated direct problem and established the existence, uniqueness, and stability of weak solutions within an appropriate functional framework, conditional on an explicit energy-inequality hypothesis (Assumption 2.1) that is a theorem in the constant-order case but is, to our knowledge, open in general for genuinely variable-order Caputo derivatives. The inverse problem was formulated as a linear operator equation, and its ill-posed nature was discussed in connection with the decay of the underlying spectral coefficients, again conditional on an explicit positivity hypothesis (Assumption 3.2) on the modal response $\Theta_n(T)$.

On the numerical side, we proposed a reconstruction method based on the conjugate gradient algorithm combined with Morozov's discrepancy principle. This approach provides an effective iterative regularization strategy that automatically adapts the stopping criterion to the noise level, and its convergence (Theorem 4.2) does not rely on Assumptions 2.1 or 3.2.

The numerical experiments carried out in one- and two-dimensional settings demonstrate that the proposed method is capable of accurately reconstructing nonsmooth source terms under different noise levels. In particular, the results show that the method remains stable and captures the main structural features of the source even in moderately noisy regimes.

The comparison between variable-order and constant-order models, performed in the one-dimensional setting for a single mild-amplitude profile, indicates that, for the configuration considered in this study, the reconstruction accuracy is primarily influenced by the noise level and the regularity of the source, while the variability of the fractional order has a secondary effect; we do not claim this observation generalizes beyond the tested configuration, and no analogous comparison was performed in two dimensions.

Future work may include: a rigorous proof (or, failing that, a precise counterexample) of Assumptions 2.1 and 3.2 for genuinely variable-order Caputo derivatives, under sharp structural conditions on $\alpha(\cdot)$; a systematic two-dimensional variable-versus-constant-order comparison and a broader sweep of variable-order profiles (amplitude and frequency); a mesh-refinement study for the variable-order L1 scheme; and the extension of the present framework to more general inverse problems, such as the simultaneous identification of time-dependent coefficients or fractional orders, as well as the incorporation of partial or boundary observations. Another promising direction is the integration of data-driven approaches, such as physics-informed neural networks, to enhance the reconstruction performance in complex and high-dimensional settings.

Funding: The authors extend their appreciation to the Deanship of Scientific Research at Northern Border University, Arar, KSA for funding this research work through the project number NBU-FFR-2026-2768-02.

Conflicts of Interest: The author declares that there are no conflicts of interest regarding the publication of this paper.

References

[1] I. Podlubny, Fractional Differential Equations: an Introduction to Fractional Derivatives, Fractional Differential Equations, to Methods of Their Solution and Some of Their Applications, Academic Press, 1998.

[2] A.A. Kilbas, H.M. Srivastava, J.J. Trujillo, Theory and Applications of Fractional Differential Equations, Elsevier Science, 2006.

[3] K. Diethelm, The Analysis of Fractional Differential Equations, Springer Berlin Heidelberg, 2010. https://doi.org/10.1007/978-3-642-14574-2.

[4] R. Metzler, J. Klafter, The Random Walk's Guide to Anomalous Diffusion: a Fractional Dynamics Approach, Phys. Rep. 339 (2000), 1–77. https://doi.org/10.1016/S0370-1573(00)00070-3.

[5] L. Caffarelli, L. Silvestre, An Extension Problem Related to the Fractional Laplacian, Commun. Partial Differ. Equ. 32 (2007), 1245–1260. https://doi.org/10.1080/03605300600987306.

[6] E. Valdinoci, From the Long Jump Random Walk to the Fractional Laplacian, arXiv:0901.3261, 2009. https://doi.org/10.48550/arXiv.0901.3261.

[7] M. Alhazmi, Y. Alrashedi, H.O. Sidi, M.O. Sidi, Detection of a Spatial Source Term within a Multi-Dimensional, Multi-Term Time-Space Fractional Diffusion Equation, Mathematics 13 (2025), 705. https://doi.org/10.3390/math13050705.

[8] S.A. Ould Ahmed Mahmoud, H. Ould Sidi, M. Ould Sidi, Determination of an Energy Source Term for Fractional Diffusion Equation, J. Sens. 2022 (2022), 7984688. https://doi.org/10.1155/2022/7984688.

[9] M.O. Sidi, H.O. Sidi, M. Alosaimi, S.A.O.A. Mahmoud, S.A.O. Beinane, H.O. Alshammari, Robin Coefficient Determination Problem in a Fractional Parabolic Differential Equation, Math. Methods Appl. Sci. 48 (2025), 52–64. https://doi.org/10.1002/mma.10257.

[10] B. Jin, W. Rundell, An Inverse Problem for a One-Dimensional Time-Fractional Diffusion Problem, Inverse Probl. 28 (2012), 075010. https://doi.org/10.1088/0266-5611/28/7/075010.

[11] J. Cheng, J. Nakagawa, M. Yamamoto, T. Yamazaki, Uniqueness in an Inverse Problem for a One-Dimensional Fractional Diffusion Equation, Inverse Probl. 25 (2009), 115002. https://doi.org/10.1088/0266-5611/25/11/115002.

[12] X.B. Yan, T. Wei, Inverse Space-Dependent Source Problem for a Time-Fractional Diffusion Equation by an Adjoint Problem Approach, J. Inverse Ill-posed Probl. 27 (2019), 1–16. https://doi.org/10.1515/jiip-2017-0091.

[13] D. Jiang, Z. Li, Coefficient Inverse Problem for Variable Order Time-Fractional Diffusion Equations from Distributed Data, Calcolo 59 (2022), 34. https://doi.org/10.1007/s10092-022-00476-3.

[14] M. Slodička, An Inverse Source Problem in a Variable-Order Time-Fractional Diffusion PDE, Mathematics 14 (2026), 488. https://doi.org/10.3390/math14030488.

[15] W. Fan, X. Hu, S. Zhu, Modelling, Analysis, and Numerical Methods for a Geometric Inverse Source Problem in Variable-Order Time-Fractional Subdiffusion, Inverse Probl. Imaging 17 (2023), 767–797. https://doi.org/10.3934/ipi.2023002.

[16] A. Alsaedi, B. Ahmad, M. Kirane, Maximum Principle for Certain Generalized Time and Space Fractional Diffusion Equations, Q. Appl. Math. 73 (2015), 163–175. https://doi.org/10.1090/S0033-569X-2015-01386-2.

[17] V. Vergara, R. Zacher, Optimal Decay Estimates for Time-Fractional and Other NonLocal Subdiffusion Equations via Energy Methods, SIAM J. Math. Anal. 47 (2015), 210–239. https://doi.org/10.1137/130941900.

[18] Y. Luchko, Maximum Principle for the Generalized Time-Fractional Diffusion Equation, J. Math. Anal. Appl. 351 (2009), 218–223. https://doi.org/10.1016/j.jmaa.2008.10.018.

[19] Y. Liu, W. Rundell, M. Yamamoto, Strong Maximum Principle for Fractional Diffusion Equations and an Application to an Inverse Source Problem, Fract. Calc. Appl. Anal. 19 (2016), 888–906. https://doi.org/10.1515/fca-2016-0048.

[20] M. Hanke, Conjugate Gradient Type Methods for Ill-Posed Problems, Chapman and Hall/CRC, 2017. https://doi.org/10.1201/9781315140193.